Correlation between structural deformation and magnetoelectric response in (1 x) Pb (Zr 0.52 Ti 0.48) O 3 – x Ni Fe 1.9 Mn 0.1 O 4 particulate composites

Rashed Adnan Islam, Jiechao Jiang, Feiming Bai, Dwight Viehland, and Shashank Priya

Citation: Applied Physics Letters **91**, 162905 (2007); doi: 10.1063/1.2799261
View online: http://dx.doi.org/10.1063/1.2799261
View Table of Contents: http://scitation.aip.org/content/aip/journal/apl/91/16?ver=pdfcov
Published by the AIP Publishing

Correlation between structural deformation and magnetoelectric response in $(1-x)$ $Pb(Zr_{0.52}Ti_{0.48})O_3-xNiFe_{1.9}Mn_{0.1}O_4$ particulate composites

Rashed Adnan Islam and Jiechao Jiang
Materials Science and Engineering, University of Texas at Arlington, Texas 76019, USA

Feiming Bai, Dwight Viehland, and Shashank Priya[a)]
Materials Science and Engineering, Virginia Tech, Blacksburg, Virginia 24061, USA

(Received 30 August 2007; accepted 25 September 2007; published online 17 October 2007)

The ferroelectric, ferromagnetic, and magnetoelectric properties of $(1-x)$ $Pb(Zr_{0.52}Ti_{0.48})O_3-xNiFe_{1.9}Mn_{0.1}O_4$ (PZT-NFM) ceramic composites were found to be dependent upon postsinter annealing and aging. It was found on annealing and aging that (i) the size and density of the NFM phase is reduced, (ii) the PZT lattice constants changed from ($a=3.87$ Å, $c=4.07$ Å) to ($a=4.07$ Å, $c=4.09$ Å), (iii) the ferroelectric and ferromagnetic Curie temperatures decreased by 8 and 33 °C, respectively, and (iv) the magnetoelectric coefficient increased by ~50%. © *2007 American Institute of Physics*. [DOI: 10.1063/1.2799261]

Single phase magnetoelectric (ME) materials (such as Cr_2O_3, $BiFeO_3$, $YMnO_3$, etc.) have two order parameters: polarization and magnetization.[1–3] However, one of the order parameters is generally large and the other small, resulting in only minor ME exchange between the two subsystems.[4,5] However, composites of magnetostrictive and piezoelectric phases are known to have a large ME product tensor property, which neither of the component phases has individually.[6–8]

In pioneering work at Philips Laboratory,[9–12] ME composites were synthesized by unidirectional solidification of a eutectic composition of $BaTiO_3$-$CoFe_2O_4$. The findings revealed ME coefficients as high as 0.13 V/cm Oe.[11] Since that time, various particulate composites of piezoelectric [$BaTiO_3$ or $Pb(Zr,Ti)O_3$] and magnetostrictive ($LiFe_5O_8$, $Ni_{1-x}Zn_xFe_2O_4$, $CoFe_2O_4$, or $CuFe_2O_4$) phases with different dimensional connectivities have been reported, such as "3-0" and "2-0."[9–18] Although the ME effect is known for various binary systems, little information is available on their phase equilibria or structural stability, limiting information concerning the mechanisms that control the magnitude of the response.[16] Investigations have shown that $NiFe_2O_4$ particles are stable in a doped-$Pb(Zr,Ti)O_3$ matrix and do not react even at sintering temperatures of up to 1250 °C.[19] Furthermore, it has been shown that postsinter thermal treatments, such as annealing and aging, enhance the ME, ferroelectric, and ferromagnetic properties of $Pb(Zr_{0.52}Tr_{0.48})O_3$ (PZT)-$NiFe_{1.9}Mn_{0.1}O_4$ (NFM).[20–22] Here, we use transmission electron microscopy to find a structural basis for these property enhancements.

Ceramic compositions with stoichiometric ratios of PZT and NFM were fabricated by a conventional mixed oxide route. Calcination of PZT and NFM powders was performed at 750 °C for 2 h and 1000 °C for 5 h, respectively. X-ray patterns of the calcined PZT and NFM powders exhibited perovskite and spinel phases. The PZT and NFM powders were then mixed together and compacted. This was followed by pressureless sintering in air at 1150 °C for 2 h, resulting in consolidated ceramic composites. Postsinter thermal treatments were then done by annealing the composites at 800 °C for 10 h, followed by quenching in air and subsequent aging at 300 °C. Samples were then diced for property measurements, electroded with Ag/Pd, and poled under a dc bias of 25 kV/cm for 20 min at 120 °C. Dielectric constant measurements were performed using a HP 4284 *LCR* meter, and magnetization versus temperature (*M-T*) curves were obtained by a Quantum Design physical properties measurement system and the ME voltage coefficient by a lock-in amplifier method. In addition, transmission electron microscopy (TEM) studies were performed using a JEOL1200 EX: both bright-field images and selected area electron diffraction (SAED) patterns were obtained.

Figure 1(a) shows a bright-field TEM image of an as-sintered sample presenting a typical microstructure. This image consists of facet phases/particles (bright contrast) embedded in the matrix. The former ones (facet phases) correspond to the NFM phase, while the latter one (matrix) corresponds to the PZT phase, as identified by the energy dispersive spectroscopy and SAED patterns. The NFM particles vary from 300 to 1500 nm. Figures 1(c) and 1(d) are SAED patterns obtained from the PZT matrix, which can be identified as the [101] and [001] zone axes of the tetragonal PZT structure, respectively. The lattice parameter of this PZT structure in the sintered sample can be determined to be $a^s_{PZT}=3.87$ Å and $c^s_{PZT}=4.07$ Å, with $c/a=1.052$, where the superscript s denotes as-sintered samples. Figures 1(e) and 1(f) are SAED patterns taken from the NFM phase in Fig. 1(a) which can be identified as the [211] and [110] zone axes of the pseudocubic structure of NFM, respectively. This pseudocubic structure has a lattice parameter of $a_{NFM}=8.42$ Å, as measured from the electron diffraction pattern. Figure 1(b) shows a bright-field TEM image of the sample annealed at 800 °C for 10 h. Figure 1(b) shows different microstructural characteristics from those shown in Fig. 1(a). The density of the NFM particles in this annealed sample is much less than that in the sintered sample. In addition, the NFM particles in the annealed sample have a typical size of 500 nm, much smaller than that in the sintered sample. The PZT phase in the annealed sample has a tetragonal structure with lattice constants of $a^a_{PZT}=4.07$ Å and $c^a_{PZT}=4.09$ Å, with $c/a=1.005$. The samples treated by annealing at

[a)]Electronic mail: spriya@vt.edu

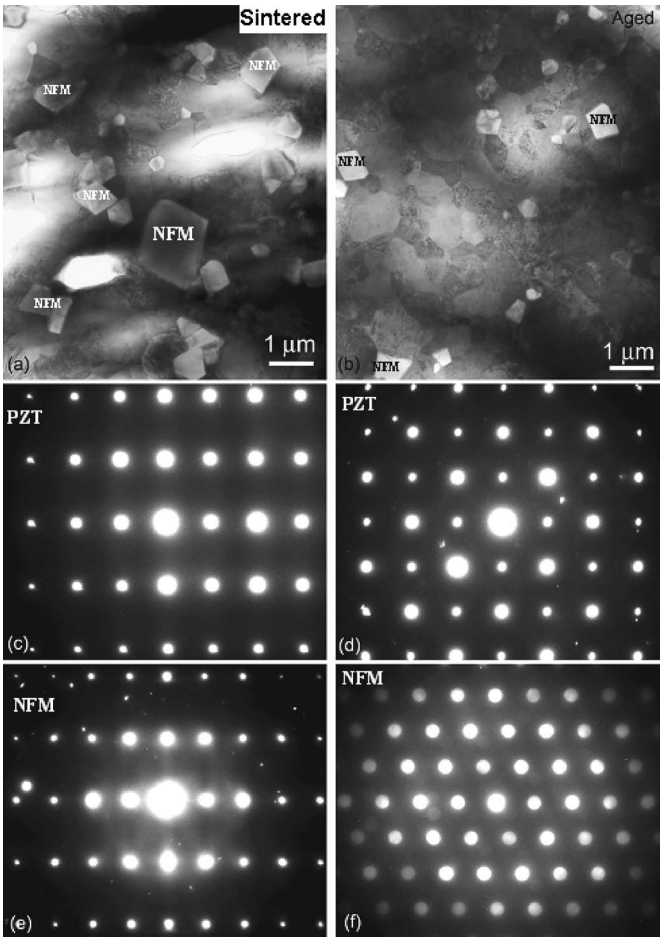

FIG. 1. Bright-field TEM images PZT-5 NFM composites after (a) sintering and (b) annealing. Selected area electron diffraction (SAED) pattern of PZT phase after sintering for (c) [101] and (d) [001] zone axes, and NFM phase after sintering for (e) [211] and (f) [110] zone axes.

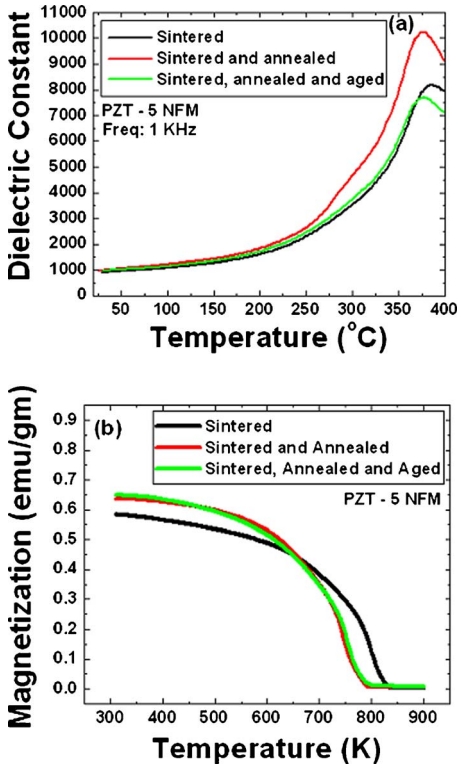

FIG. 2. (Color online) Temperature dependent ferroelectric and ferromagnetic properties of PZT-5 NFM composite. Temperature dependent (a) dielectric constant and (b) saturation magnetization.

800 °C for 10 h, followed by quenching in air and subsequent aging at 300 °C show similar microstructure to the annealed sample shown in Fig. 1(b), but the density of the NFM phase was further reduced. The above results demonstrate that the postsinter thermal treatments at 800 °C for 10 h results in the reduction of the NFM phase by diffusing into the PZT structure. Meanwhile, the PZT phase transfers from the tetragonal structure to a pseudocubic structure with larger lattice constants.

Another noticeable feature observed was that in the sintered sample due to the presence of a large amount of defects, the grain boundaries are diffused. During annealing, as the structure finds more time to reduce the defects from its structure, sharp grain boundaries were observed. The defects in the boundary layers disrupt or weaken the interatomic bonds, they reduce the effective elastic moduli of the boundary layers resulting in their elastic softening. Such a softening is expected to impair a "transfer" of the elastic strain generated in one grain to another and thus should have a detrimental effect on the ME coupling of these grains. Removal of the defects and shrinkage of the grain boundary layers in the equilibration process during annealing restores the interatomic bonding.

Figures 2(a) and 2(b) show the dielectric constant and magnetization as a function of temperature for a PZT-5 at. % NFM composite. Data are shown in each figure for the three different thermal conditions. The ferroelectric Curie temperature, as identified by the temperature of the maximum in the dielectric constant, was only decreased slightly (~8 °C) by annealing and aging. However, the ferromagnetic one was decreased notably more: from 828 K in the as-sintered condition to 788 K after annealing. In addition, it should be noted that the saturation magnetization at room temperature was increased from about 0.58 to 0.64 emu/g after annealing. This modest change in magnetization after annealing at 800 °C may be related to a Mn valence change in the ferrite phase. Previously, it has been shown that $Mn^{+3} \rightarrow Mn^{+2}$ begins to occur for temperatures above 700 °C,[23] resulting in an adjustment in the stoichiometry of the ferrite phase to $[Ni(Mn)_y]Fe_{1.9}Mn_{(0.1-y)}O_4$ where y is the concentration of Mn^{+2}. On quenching, this adjusted stoichiometry will be metastably frozen in to room temperature. Since Mn^{+2} has a higher magnetic moment than Mn^{+3}, it is reasonable to expect a slight increase in saturation magnetization after annealing.[24]

Finally, we show the ME voltage coefficient for $x=3$, 5, and 10 at. % as given in Figs. 3(a)–3(c), respectively. Data are given in each figure for the three different thermal histories. These results show that the ME voltage coefficient is increased by annealing and aging. Please note that these values are lower than the ones previously reported[20,22] for the same compositions. For $x=10$ at.%, the ME coefficient was increased from 60 to 88 mV/cm Oe by annealing and aging: nearly a 50% increase. We attribute this increase to the expansion of the lattice constants in the PZT phase and reduction of defects at that interphase interfaces after annealing. The presence of defects at the interfaces would decrease the ability of piezoelectric phase regions to elastically respond to strictions imposed on it by neighboring magnetostrictive ones, or vice versa. To achieve high ME properties, the

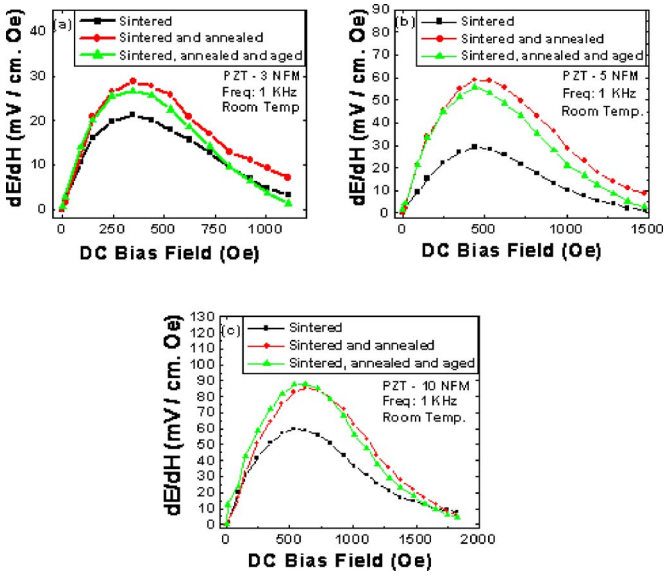

FIG. 3. (Color online) Magnetoelectric coefficient for different composites at three different conditions: (a) PZT-3 NFM, (b) PZT-5 NFM, and (c) PZT-10 NFM.

boundary conditions between phases need to be as mechanically free as possible. Contributions to the enhancements in the ME coefficient may also result from increased magnetization from $Mn^{+3} \rightarrow Mn^{+2}$, as an enhanced magnetic permeability has been reported to increase the effective piezomagnetic coefficient $(d\lambda/dH)$.[25]

In summary, we report a correlation between structural deformation in PZT matrix, the presence of defects between component phases in piezoelectric-magnetostrictive composites, and the change in magnetization with changes in the ME coefficient. It was found that a considerable amount of lattice constant expansion in the PZT structure, removal of defects, and increase in magnetization contribute to the enhancement in ME coefficient after annealing and aging.

The authors acknowledge the support from the Office of Basic Energy Science, DOE, through Grant No. DE-FG02-06ER46288.

[1]D. N. Astrov, Sov. Phys. JETP **11**, 708 (1960).
[2]J. Wang, J. B. Neaton, H. Zheng, V. Nagarajan, S. B. Ogale, B. Liu, D. Viehland, V. Vathiyanathan, D. G. Schlom, U. V. Waghmare, N. A. Spaldin, K. M. Rabe, M. Wuttig, and R. Ramesh, Science **299**, 1719 (2003).
[3]B. B. Van Aken, T. T. A. Palstra, A. Filippetti, and N. A. Spaldin, Nat. Mater. **3**, 164 (2004).
[4]C. G. Duan, S. S. Jaswal, and E. Y. Tsymbal, Phys. Rev. Lett. **97**, 047201 (2006).
[5]M. Fiebig, T. Lottermoser, D. Frohllch, A. V. Goltsev, and R. V. Pisarev, Nature (London) **419**, 818 (2002).
[6]M. Zheng, J. G. Wan, Y. Wang, H. Yu, J. M. Liu, X. P. Jiang, and C. W. Nan, J. Appl. Phys. **95**, 8069 (2004).
[7]J. Ryu, A. V. Carazo, K. Uchino, and H. Kim, J. Electroceram. **7**, 17 (2001).
[8]V. C. Flores, D. B. Baques, D. C. Flores, and J. A. M. Aquino, J. Appl. Phys. **99**, 08J503 (2006).
[9]J. V. D. Boomgaard, A. M. J. G. Van Run, and J. V. Suchtelen, Ferroelectrics **10**, 295 (1976).
[10]J. V. D. Boomgaard and R. A. J. Born, J. Mater. Sci. **13**, 1538 (1978).
[11]J. V. D. Boomgaard, D. R. Terrell, R. A. J. Born, and H. F. J. I. Giller, J. Mater. Sci. **9**, 1705 (1974).
[12]A. M. J. G. Van Run, D. R. Terrell, and J. H. Scholing, J. Mater. Sci. **9**, 1710 (1974).
[13]T. G. Lupeiko, I. V. Lisnevskaya, M. D. Chkheidze, and B. I. Zvyagintsev, Inorg. Mater. **31**, 1139 (1995).
[14]T. G. Lupeiko, I. B. Lopatina, S. S. Lopatin, and I. P. Getman, Neorg. Mater. **27**, 2394 (1991).
[15]T. G. Lupeiko, I. B. Lopatina, I. V. Kozyrev, and L. A. Derbaremdiker, Neorg. Mater. **28**, 632 (1991).
[16]Y. I. Bokhan and V. M. Laletin, Inorg. Mater. **32**, 634 (1996).
[17]T. G. Lupeiko, S. S. Lopatin, I. V. Lisnevskaya, and B. I. Zvyagintsev, Inorg. Mater. **30**, 1353 (1994).
[18]Y. R. Dai, P. Bao, J. S. Zhu, J. G. Wan, H. M. Shen, and J. M. Liu, J. Appl. Phys. **96**, 5687 (2004).
[19]W. E. Kramer, R. H. Hopkins, and M. R. Daniel, J. Mater. Sci. Lett. **12**, 409 (1977).
[20]R. A. Islam and S. Priya, Integr. Ferroelectr. **82**, 1 (2006).
[21]R. A. Islam and S. Priya, Jpn. J. Appl. Phys., Part 2 **45**, L128 (2006).
[22]R. A. Islam and S. Priya, Int. J. Appl. Ceram. Technol. **3**, 353 (2006).
[23]Z. J. Zhang, Z. L. Wang, B. C. Chakoumakos, and J. S. Yin, J. Am. Chem. Soc. **120**, 1800 (1998).
[24]C. Rath, S. Anand, R. P. Das, K. K. Sahu, S. D. Kulkarni, S. K. Date, and N. C. Mishra, J. Appl. Phys. **91**, 2211 (2002).
[25]S. Dong, J. Zhai, J. F. Li, and D. Viehland, J. Appl. Phys. **100**, 124108 (2006).